Available online at www.sciencedirect.com
ScienceDirect
Biochemical and Biophysical Research Communications 360 (2007) 464–469
BBRC
www.elsevier.com/locate/ybbrc

Endogenous metalloprotease solubilizes IL-13 receptor α2 in airway epithelial cells ☆

Mikiko Matsumura [a], Hiromasa Inoue [a,*], Takafumi Matsumoto [a], Takako Nakano [a], Satoru Fukuyama [a], Koichiro Matsumoto [a], Koichi Takayama [a], Makoto Saito [b], Koji Kawakami [c], Yoichi Nakanishi [a]

[a] *Research Institute for Diseases of the Chest, Graduate School of Medical Sciences, Kyushu University, 3-1-1 Maidashi, Higashi-ku, Fukuoka 812-8582, Japan*
[b] *Laboratory of Molecular Biology of Infectious Agents, Graduate School of Biomedical Sciences, Nagasaki University, 1-14 Bunkyo-machi, Nagasaki 852-8521, Japan*
[c] *Department of Pharmacoepidemiology, School of Medicine and Public Health, Kyoto University, Yoshida Konoecho, Sakyoku, Kyoto 606-8501, Japan*

Received 7 June 2007
Available online 19 June 2007

Abstract

IL-13 receptor α2 (IL-13Rα2) has been postulated to be a decoy receptor. The precise mechanisms for the generation of soluble IL-13Rα2 and the biological activity of the endogenous soluble form have not been reported. Hypothesizing that the soluble form of IL-13Rα2 is generated by proteolytic cleavage of membrane-bound receptors, we transfected human airway epithelial cells with adenoviral vectors encoding full-length IL-13Rα2. Eotaxin production from IL-13Rα2-transfected cells was suppressed, and soluble IL-13Rα2 in the supernatants was increased time-dependently after the transfection. The transfer of conditioned media from IL-13Rα2-transfected cells inhibited IL-13-induced eotaxin production and STAT6 phosphorylation in non-transfected cells. PMA enhanced the release of soluble IL-13Rα2, and metalloprotease inhibitors inhibited this release. These findings suggest that airway epithelial cells with upregulation of membrane-bound IL-13Rα2 secrete soluble IL-13Rα2 into its supernatant, causing the autocrine and paracrine downregulation of the IL-13/STAT6 signal. Metalloprotease(s) are responsible for the proteolytic cleavage of cell surface IL-13Rα2.

Keywords: Th2 cytokine; Soluble receptor; Protease; Phorbol 12-myristate 13-acetate

Interleukin (IL)-13, a type 2 helper T (Th2) cytokine, plays important role in asthma by enhancing the recruitment of eosinophils, stimulating IgE-producing B cells, and directly inducing airway hyperresponsiveness [1–3]. IL-13 mediates its effects via a complex receptor system including IL-4Rα, IL-13Rα1, and IL-13Rα2. IL-13 binds to the primary receptor IL-13Rα1 chain with low affinity [4,5]. However, with the IL-4Rα chain, IL-13Rα1 binds IL-13 with high affinity and results in the activation of the janus-activated kinase (JAK)-STAT pathway [6]. IL-13 also binds to a second receptor, IL-13Rα2, but with high affinity [7,8].

The IL-13Rα2 chain has not been shown to mediate signaling through the JAK-STAT pathway [9,10] because its short cytoplasmic region (17 amino acids in the human) does not contain an obvious signaling motif or JAK-STAT binding sequence [8]. IL-13Rα2 knockout mice showed enhanced IL-13 responses [11,12]; therefore, IL-13Rα2 has been postulated to be a decoy receptor. Recently, it has been demonstrated that IL-13-induced TGF-β1-mediated fibrosis depends on IL-13Rα2 signals through the AP-1 pathway, and IL-13Rα2 may also contribute to IL-13 responses [13].

☆ This work was supported in part by Grant-in-Aid for Scientific Research from the Japan Society for the Promotion of Science.
* Corresponding author. Fax: +81 92 642 5389.
E-mail address: inoue@kokyu.med.kyushu-u.ac.jp (H. Inoue).

0006-291X/$ - see front matter © 2007 Elsevier Inc. All rights reserved.
doi:10.1016/j.bbrc.2007.06.076

IL-13Rα2 has been shown to be predominantly an intracellular molecule mobilized to the cell surface from intracellular stores [14]. The extracellular domain of IL-13Rα2 could be cleaved. The overexpression of the IL-13Rα2 extracellular domain inhibits the biological activity of IL-13 [15]. The precise mechanism of the generation of soluble IL-13Rα2 is unclear, however, and the inhibitory action of the soluble form after the enhanced expression of the full-length IL-13Rα2 chain has not yet been reported.

Soluble cytokine receptors can be generated by several mechanisms, including the proteolytic cleavage of membrane-bound receptor proteins from the cell surface and alternative splicing of mRNA transcripts [16]. The release of the soluble proteins can be strongly stimulated by phorbol ester PMA, a potent activator of protein kinase C [17]. We examined whether the transfection with the full-length IL-13Rα2 chain to human airway epithelial cells increases the generation of soluble IL-13Rα2, and we studied the inhibitory effects of the soluble form on IL-13 response. We also stimulated the cells with PMA after full-length IL-13Rα2 transfection and examined the effect of protease inhibitors in order to characterize the release of soluble IL-13Rα2.

Materials and methods

Cell culture. BEAS-2B cells, a human airway epithelial cell line transformed with the SV40 virus, were cultured in DMEM/F-12 medium with 10% FBS, penicillin, and streptomycin.

Adenovirus transfection and stimulation. A replication-defective ΔE1ΔE3 adenoviral vector expressing the IL-13Rα2 chain gene under the CMV promoter (Ad-IL-13Rα2) was constructed as described previously [18]. Another replication-defective adenoviral vector expressing the β-galactosidase gene (Ad-LacZ) was constructed in the same way and utilized as an adenoviral infection control.

BEAS-2B cells were seeded in 6-well tissue culture plates until subconfluence and infected with Ad-LacZ or Ad-IL-13Rα2 diffused in DMEM/F12 medium with 2% FBS for 2 h. Cells were washed and cultured in DMEM/F12 medium with 10% FBS as indicated in each experiment. Then, after 2 h of serum starvation, the cells were stimulated with human rIL-13.

Supernatants were collected at 72 h after transfection and concentrated to about one-seventh of the original volume by centrifugal filtration through the MW 10,000 cutoff membrane (Millipore, Bedford, MA). Other cells were stimulated with human rIL-13 dissolved in concentrated medium.

To remove remaining IL-13Rα2 vectors in supernatants, trypsin was used 2 h after transfection, and the cells were re-seeded in culture dishes.

Measurement of eotaxin and soluble IL-13Rα2. The concentrations of eotaxin were measured in the cell supernatant fluids from BEAS-2B using ELISA [19]. The minimum concentration detected by this method was 5 pg/ml. Quantification of human-soluble IL-13Rα2 expression was done with ELISA (R&D Systems).

Analysis of effect of PMA on release of soluble IL-13Rα2. After 2 h of serum starvation, cells were treated with stimuli as indicated in each experiment. For inhibitor studies, serum-starved cells were pretreated with inhibitors for 30 min before exposure to stimuli. In studies of PMA, cells were treated with PMA (10 ng/ml) for 2 h. Supernatants were collected for the measurement of soluble IL-13Rα2 by ELISA.

Western blotting analysis. After cytokine treatment, protein extracts from the cells were prepared with lysis buffer. Immunoblotting was performed using anti-phospho STAT6, or anti-STAT6 antibodies, as described [19,20].

RT-PCR analysis. Total RNA was isolated, and reverse transcription (RT)-polymerase chain reaction (PCR) was performed on 1.0 μg total RNA. An oligo (dT) primer was used for RT, and cDNA was amplified by PCR using specific primers. The following primer pairs specific for IL-13Rα2 and for β-actin were used: 5′-AATGGCTTTCGTTTGCTTGG-3′ and 5′-ACGCAATCCATATCCTGAAC-3′; and 5′-TCCTGTGGCA TCCATGAAACT-3′ and 5′-GAAGCACTTGCGGTGCACGAT-3′, respectively. Amplification was performed as previously reported [19].

Data analysis. Values are expressed as means ± SEM. Differences between groups were analyzed by ANOVA, and the significance of differences between values was assessed with the Bonferroni correction. A P value below 0.05 was considered significant.

Results

IL-13Rα2 gene induction in airway epithelial cells and secretion of soluble L-13Rα2

IL-13Rα2 mRNA levels were barely detectable in BEAS-2B cells. To establish airway epithelial cells with a high expression of IL-13Rα2, BEAS-2B cells were transfected with a full-length IL-13Rα2 using Ad-IL-13Rα2. Ad-IL-13Rα2 transfection, but not Ad-LacZ, induced IL-13 Rα2 mRNA in a multiplicity of infection (moi)-dependent manners (Fig. 1A). Maximal induction of IL-13Rα2 was observed at 30-moi transfection of Ad-IL-13Rα2. We also analyzed the time kinetics of IL-13Rα2 mRNA expression. The high levels of IL-13Rα2 mRNA expression were sustained for 24–48 h after transfection in BEAS-2B cells (Fig. 1B). To confirm the IL-13Rα2 protein on the surface of IL-13Rα2-transfected cells, flow cytometric analysis was performed using the FITC-conjugated antibody against the human IL-13Rα2 chain. IL-13Rα2 expression was detected at the surface of BEAB-2B cells transfected with Ad-IL-13Rα2 but not with Ad-LacZ (data not shown).

IL-13 induces eotaxin in the airways STAT6-dependently [21,22], and IL-13Rα2 has been reported to limit IL-13-mediated responses through the JAK/STAT6 pathway as a "decoy" receptor [9,12,23]. To confirm the function of overexpressed membrane IL-13Rα2 in airway epithelial cells, we analyzed eotaxin production and STAT6 phosphorylation induced by IL-13. Transfection of Ad-IL-13Rα2, but not of Ad-LacZ, inhibited IL-13-induced STAT6 activation (data not shown) and eotaxin production in BEAS-2B cells (Fig. 1C), suggesting that the overexpression of IL-13Rα2 on the surface of airway epithelial cells leads to the inhibition of STAT6-dependent signals in the cells.

To test whether a soluble form of IL-13Rα2 is secreted after IL-13Rα2 transduction, BEAS-2B cells were transduced with 30-moi Ad-IL-13Rα2, and the concentration of soluble IL-13Rα2 in the supernatant of the cells was measured by ELISA. There was a time-dependent increase in the level of soluble IL-13Rα2 in the conditioned media, indicating the spontaneous release of soluble IL-13Rα2

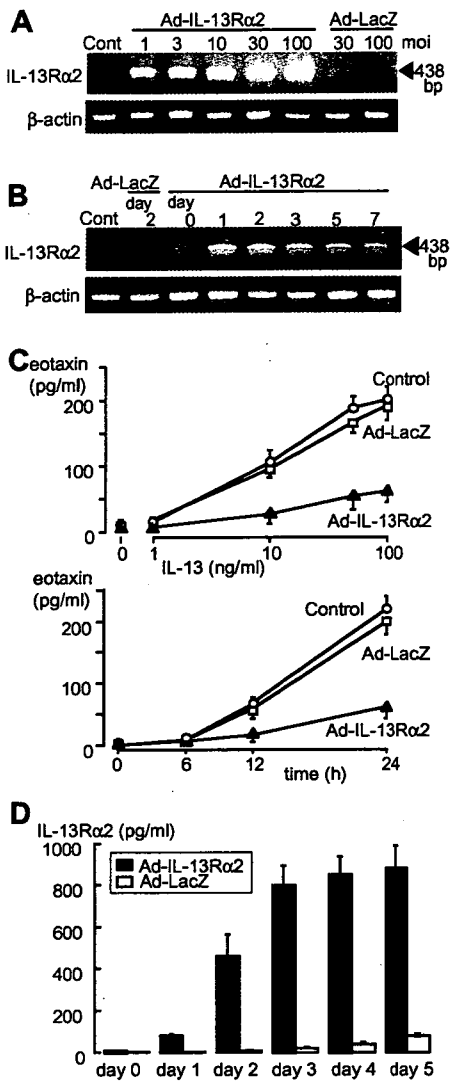

Fig. 1. Effects of transfection with a full-length IL-13Rα2 using adenoviral vectors (Ad-IL-13Rα2) on IL-13Rα2 expression, IL-13-induced eotaxin production, and soluble IL-13Rα2 secretion from airway epithelial cells. (A) BEAS-2B cells were transfected with Ad-IL-13Rα2 or the control adenoviral vector (Ad-LacZ) at the indicated multiplicity of infection (moi). The total RNA was isolated from the cells 3 days after the transfection or from untransfected cells (Cont), and IL-13Rα2 levels were amplified by RT-PCR. RT-PCR products for β-actin are shown for comparison. Amplified DNA was separated by electrophoresis on an agarose gel containing ethidium bromide, illuminated with ultraviolet light, and photographed. (B) BEAS-2B cells were transfected with Ad-IL-13Rα2 or Ad-LacZ (30 moi). On the indicated days after transfection, total RNA was isolated from the cells, and IL-13Rα2 levels were amplified by RT-PCR. (C) Dose-dependent and time-dependent eotaxin production from untransfected (Cont), Ad-IL-13Rα2 (30 moi)-transfected, or Ad-LacZ (30-moi)-transfected BEAS-2B cells 24 h after stimulation with IL-13 (left), or the indicated time after IL-13 stimulation (50 ng/ml, right). Values are means ± SEM, $n = 5$. (D) After transfection with Ad-IL-13Rα2 or Ad-LacZ (30 moi), soluble IL-13Rα2 in the supernatant of BEAS-2B cells was quantified by ELISA. Values are means ± SEM, $n = 5$.

from the cell surface after full-length IL-13Rα2 transfection (Fig. 1D).

Functional analysis of soluble IL-13Rα2

We next examined the inhibitory effects of soluble IL-13Rα2 on IL-13-induced eotaxin expression. The transfer of the 3-day cell culture media (referred to as conditioned media) to other un-transfected BEAS-2B cells slightly but significantly attenuated IL-13-induced eotaxin production (Fig. 2A). The transfer of the cell culture media collected just after the transfection to other un-transfected BEAS-

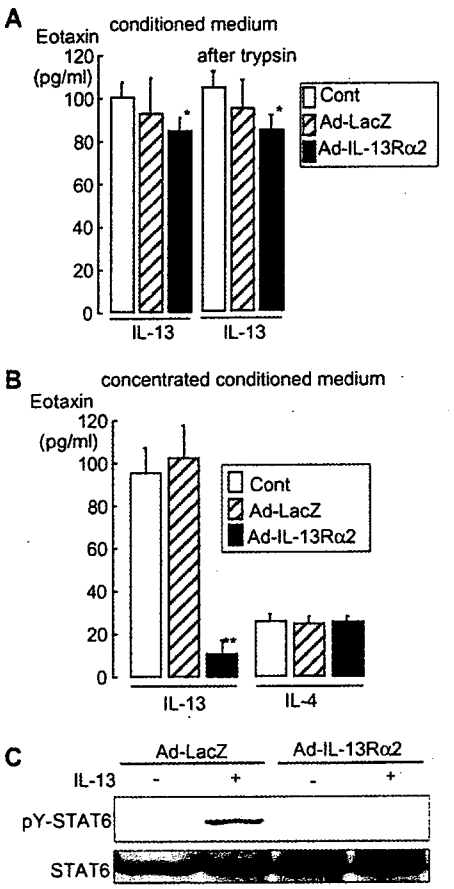

Fig. 2. Soluble IL-13Rα2 suppresses IL-13-induced eotaxin expression and STAT6 activation in human airway epithelial cells. (A) Three days after the transfection of Ad-IL-13Rα2 (30-moi) or Ad-LacZ (30-moi), the overlying cell culture medium (conditioned medium) was removed. The conditioned medium was transferred to untransfected BEAS-2B cells and stimulated with IL-13 (10 ng/ml) for 24 h. Eotaxin levels in the supernatant were measured. Values are means ± SEM, $n = 5$. $^{*}P < 0.05$; $^{**}P < 0.01$, compared with conditioned media from untransfected cells. (B) Three days after the transfection of Ad-IL-13Rα2 (30 moi) or Ad-LacZ (30 moi), the overlying cell culture medium (conditioned medium) was removed. The concentrated conditioned medium (one-seventh of the original volume) was transferred to untransfected BEAS-2B cells and stimulated with IL-13 (10 ng/ml) or IL-4 (10 ng/ml) for 24 h. Eotaxin levels in the supernatant were measured. Values are means ± SEM, $n = 5$. $^{*}P < 0.05$; $^{**}P < 0.01$, compared with concentrated conditioned media from untransfected cells. (C) The concentrated conditioned medium was transferred to untransfected BEAS-2B cells and stimulated with IL-13 (10 ng/ml) for 30 min. Cell extracts were immunoblotted with the indicated antibodies.

2B cells did not affect IL-13-induced eotaxin production. Furthermore, Ad-IL-13Rα2-transfected cells were re-seeded after trypsin treatment to remove Ad-IL-13Rα2 vectors, and the concentrated 3-day cell culture media of re-seeded cells also inhibited IL-13-induced eotaxin production in other cells (Fig. 2A). These results suggest that an inhibitory effect of cell culture media is not due to re-transfection of Ad-IL-13Rα2.

Conditioned media were then concentrated to about one-seventh of the original volume by centrifugal filtration. The transfer of the concentrated 3-day conditioned media to un-transfected BEAS-2B cells markedly inhibited STAT6 phosphorylation and eotaxin production induced by IL-13 (Fig. 2B and C). The transfer of the concentrated conditioned media did not affect IL-4-induced eotaxin production from BEAS-2B cells. These findings suggest that soluble mediator(s) released after IL-13Rα2 transfection inhibit IL-13-induced eotaxin expression in epithelial cells.

Effect of protease inhibitor and PMA on soluble IL-13Rα2 release

Because a full-length IL-13Rα2 gene was transfected to the cells, the detection of IL-13Rα2 in the cell culture medium may implicate the generation of soluble IL-13Rα2 by the proteolytic cleavage of surface receptors. In most cases of the proteolytic cleavage of surface receptors, PMA stimulates the release of soluble proteins [24], and many PMA-induced shedding events have been known to be mediated by metalloproteases such as the TNFα-converting enzyme (TACE), a member of "a disintegrin and metalloprotease (ADAM)" family [16]. Therefore, we tested the effect of PMA on the release of soluble IL-13Rα2 and whether the PMA-induced release of IL-13Rα2 is sensitive to the metalloprotease inhibitor GM6001, to the TACE inhibitor TNFα protease inhibitor-1 (TAPI-1), or to other protease inhibitors. The release of soluble IL-13Rα2 into the supernatant was strongly accelerated by the treatment of the cells with PMA, and vehicle did not affect soluble IL-13Rα2. This PMA-induced release of soluble IL-13Rα2 was markedly inhibited by GM6001 or by TAPI-1 (Fig. 3). Serine protease inhibitor (aprotinin), cysteine protease inhibitor (leupeptin), or amniopeptidase B inhibitor (bestatin) did not affect the PMA-induced release of IL-13Rα2 (Fig. 3). These findings imply that endogenous metalloprotease(s) activate the solubilization of IL-13Rα2.

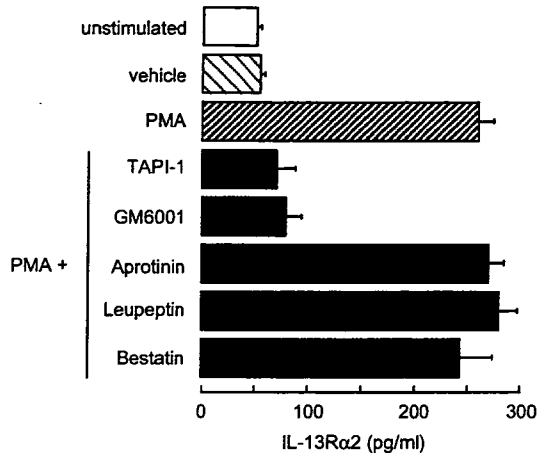

Fig. 3. Inhibition of soluble IL-13Rα2 generation from Ad-IL-13Rα2 transfected cells by protease inhibitors. Transfected BEAS-2B cells (Ad-IL-13Rα2, 30 moi) were pretreated with TAP-1 (30 μM), GM6001 (10 μM), aprotinin (1 μM), leupeptin (100 μM), or bestatin (10 μM) for 30 min and then stimulated with PMA (10 ng/ml) for 2 h. Supernatants were collected for the measurement of soluble IL-13Rα2 by ELISA. Values are means ± SEM, $n = 3$.

Discussion

We demonstrate that the transfection of full-length IL-13Rα2 induces the release of soluble IL-13Rα2 from airway epithelial cells and that the transfer of conditioned media from IL-13Rα2-transfected cells inhibits IL-13-induced eotaxin production and STAT6 phosphorylation in other non-transfected cells. PMA enhances the release of soluble IL-13Rα2, and metalloprotease inhibitors block this PMA-induced release of IL-13Rα2. These findings suggest that the upregulation of membrane-bound IL-13Rα2 in airway epithelial cells secretes soluble IL-13Rα2 into its supernatant, leading to downregulation of the IL-13/STAT6 signal, and that a group of endogenous metalloproteases is responsible for the generation of soluble IL-13Rα2.

Soluble IL-13Rα2 might be generated by some mechanisms, including the proteolytic cleavage of a membrane-bound receptor and the alternative splicing of mRNA transcripts in humans. Many PMA-induced releases of soluble receptors have been known to be mediated by metalloproteases [16]. In the present study, the PMA-induced release of endogenous IL-13Rα2 is blocked by metalloprotease inhibitors in airway epithelial cells. Matrix metalloproteinases, membrane-tethered matrix metalloproteinases, and zinc-dependent ADAM family metalloproteinases have been shown to be responsible for the cleavage of the majority of shed proteins [25]. Among these, members of the ADAM family are particularly important [25,26]. TACE (ADAM17) has surfaced recently as a central mammalian ectodomain sheddase [26], and TACE acts on ectodomain cleavage and shedding of cytokine receptors, such as TNF receptors, the IL-6R α-chain, and the IL-15 α-chain [16]. IL-13 is a potent inducer of a variety of MMP moieties, including MMP-2, -8, -9, -12, -13, and -14 [27,28]. MMP-12 has an inhibitory role on eosinophil and macrophage accumulation in the generation of IL-13-induced inflammation, while MMP-9 inhibits neutrophil accumulation [29]. MMP-9 and MMP-12 can be considered downstream mediators and regulators of the IL-13-induced inflammatory response. The expression and/or activation of metalloproteinases, including TACE, might be also regulated by IL-13. Deregulation of metalloproteinases and soluble IL-13Rα2 secretion may take part in the pathophysiology of asthma.

The soluble form of IL-13Rα2 is reported to be generated by alternative splicing in the murine system [30]. In this report, however, several mouse organs expressed two IL-13Rα2 transcripts: the longer full-length protein and the shorter transcript lacking the transmembrane region exon10. Conditioned medium from transfectants expressing only the full-length transcript did contain detectable soluble IL-13Rα2, although the levels were lower than those of the transfectants expressing the shorter transcript [30]. These results indicate that the generation of soluble IL-13Rα2 can occur from the cleavage of membrane IL-13Rα2 in addition to an alternative transcript encoding a soluble form.

It has been reported that the release of an exosome-like vesicle acts as an alternative mechanism for the generation of soluble TNF receptor 1 [31]. Conditioned medium of epithelial cells after the transfection of IL-13Rα2 might contain full-length IL-13Rα2 in exosome-like vesicles. In the present study, PMA stimulated the release of IL-13Rα2 and metalloprotease inhibitors inhibited this release, suggesting that an increase in IL-13Rα2 in conditioned media is due to the proteolytic cleavage of the membrane-bound receptor but not due to the release of exosome-like vesicles.

IL-13Rα2 exists intracellularly, on the cell-surface membrane, and in soluble form. Although it has been shown that surface IL-13Rα2 is spontaneously released into the medium [32], the inhibitory action of the soluble form after enhanced expression of the full-length IL-13Rα2 chain has not yet been certified. In the present study, we demonstrate that airway epithelial cells after the upregulation of surface IL-13Rα2 release soluble IL-13Rα2, indicating that soluble IL-13Rα2 is a transferable inhibitor of IL-13 response in the human system.

In summary, we found that the airway epithelial cells with upregulation of membrane-bound IL-13Rα2 secrete biologically active soluble IL-13Rα2, which can effectively inhibit IL-13/STAT6 signals. A group of endogenous metalloproteases is responsible for the generation of soluble IL-13Rα2. Allergic airway inflammation may modulate the expression of these proteases and their inhibitors in addition to IL-13Rα2 expression. Further studies are warranted to further elucidate the mechanisms that regulate the generation of soluble IL-13Rα2.

Acknowledgments

We thank Ayako Hashizume, Tomoko Yoshimura, Yuki Yoshiura, and the Morphology Core, Faculty of Medicine, Kyushu University, for technical assistance.

References

[1] G. Grunig, M. Warnock, A.E. Wakil, R. Venkayya, F. Brombacher, D.M. Rennick, D. Sheppard, M. Mohrs, D.D. Donaldson, R.M. Locksley, D.B. Corry, Requirement for IL-13 independently of IL-4 in experimental asthma, Science 282 (1998) 2261–2263.

[2] M. Wills-Karp, J. Luyimbazi, X. Xu, B. Schofield, T.Y. Neben, C.L. Karp, D.D. Donaldson, Interleukin-13: central mediator of allergic asthma, Science 282 (1998) 2258–2261.

[3] Z. Zhu, R.J. Homer, Z. Wang, Q. Chen, G.P. Geba, J. Wang, Y. Zhang, J.A. Elias, Pulmonary expression of interleukin-13 causes inflammation, mucus hypersecretion, subepithelial fibrosis, physiologic abnormalities, and eotaxin production, J. Clin. Invest. 103 (1999) 779–788.

[4] M.J. Aman, N. Tayebi, N.I. Obiri, R.K. Puri, W.S. Modi, W.J. Leonard, cDNA cloning and characterization of the human interleukin 13 receptor alpha chain, J. Biol. Chem. 271 (1996) 29265–29270.

[5] D.J. Hilton, J.G. Zhang, D. Metcalf, W.S. Alexander, N.A. Nicola, T.A. Willson, Cloning and characterization of a binding subunit of the interleukin 13 receptor that is also a component of the interleukin 4 receptor, Proc. Natl. Acad. Sci. USA 93 (1996) 497–501.

[6] B. Miloux, P. Laurent, O. Bonnin, J. Lupker, D. Caput, N. Vita, P. Ferrara, Cloning of the human IL-13R alpha1 chain and reconstitution with the IL4R alpha of a functional IL-4/IL-13 receptor complex, FEBS Lett. 401 (1997) 163–166.

[7] D. Caput, P. Laurent, M. Kaghad, J.M. Lelias, S. Lefort, N. Vita, P. Ferrara, Cloning and characterization of a specific interleukin (IL)-13 binding protein structurally related to the IL-5 receptor alpha chain, J. Biol. Chem. 271 (1996) 16921–16926.

[8] D.D. Donaldson, M.J. Whitters, L.J. Fitz, T.Y. Neben, H. Finnerty, S.L. Henderson, R.M. O'Hara Jr., D.R. Beier, K.J. Turner, C.R. Wood, M. Collins, The murine IL-13 receptor alpha 2: molecular cloning, characterization, and comparison with murine IL-13 receptor alpha 1, J. Immunol. 161 (1998) 2317–2324.

[9] K. Kawakami, J. Taguchi, T. Murata, R.K. Puri, The interleukin-13 receptor alpha2 chain: an essential component for binding and internalization but not for interleukin-13-induced signal transduction through the STAT6 pathway, Blood 97 (2001) 2673–2679.

[10] K. Kawakami, F. Takeshita, R.K. Puri, Identification of distinct roles for a dileucine and a tyrosine internalization motif in the interleukin (IL)-13 binding component IL-13 receptor alpha 2 chain, J. Biol. Chem. 276 (2001) 25114–25120.

[11] M.G. Chiaramonte, M. Mentink-Kane, B.A. Jacobson, A.W. Cheever, M.J. Whitters, M.E. Goad, A. Wong, M. Collins, D.D. Donaldson, M.J. Grusby, T.A. Wynn, Regulation and function of the interleukin 13 receptor alpha 2 during a T helper cell type 2-dominant immune response, J. Exp. Med. 197 (2003) 687–701.

[12] N. Wood, M.J. Whitters, B.A. Jacobson, J. Witek, J.P. Sypek, M. Kasaian, M.J. Eppihimer, M. Unger, T. Tanaka, S.J. Goldman, M. Collins, D.D. Donaldson, M.J. Grusby, Enhanced interleukin (IL)-13 responses in mice lacking IL-13 receptor alpha 2, J. Exp. Med. 197 (2003) 703–709.

[13] S. Fichtner-Feigl, W. Strober, K. Kawakami, R.K. Puri, A. Kitani, IL-13 signaling through the IL-13alpha(2) receptor is involved in induction of TGF-beta(1) production and fibrosis, Nat. Med. (2005).

[14] M.O. Daines, G.K. Hershey, A novel mechanism by which interferon-gamma can regulate interleukin (IL)-13 responses. Evidence for intracellular stores of IL-13 receptor alpha -2 and their rapid mobilization by interferon-gamma, J. Biol. Chem. 277 (2002) 10387–10393.

[15] M. Kioi, S. Seetharam, R.K. Puri, N-linked glycosylation of IL-13R alpha2 is essential for optimal IL-13 inhibitory activity, FASEB J. 20 (2006) 2378–2380.

[16] S.J. Levine, Mechanisms of soluble cytokine receptor generation, J. Immunol. 173 (2004) 5343–5348.

[17] Y. Nishizuka, Studies and perspectives of protein kinase C, Science 233 (1986) 305–312.

[18] M. Saito, T. Murata, K. Watanabe, K. Kawakami, M. Suzuki, T. Koji, R.K. Puri, K. Kitazato, N. Kobayashi, Adenoviral vector-mediated gene transfer of IL-13Ralpha2 chain followed by IL-13 cytotoxin treatment offers potent targeted therapy for cytotoxin-resistant cancers, Int. J. Cancer 116 (2005) 1–8.

[19] T. Nakano, H. Inoue, S. Fukuyama, K. Matsumoto, M. Matsumura, M. Tsuda, T. Matsumoto, H. Aizawa, Y. Nakanishi, Niflumic acid

suppresses interleukin-13-induced asthma phenotypes, Am. J. Respir. Crit. Care Med. 173 (2006) 1216–1221.
[20] H. Inoue, R. Kato, S. Fukuyama, A. Nonami, K. Taniguchi, K. Matsumoto, T. Nakano, M. Tsuda, M. Matsumura, M. Kubo, F. Ishikawa, B.G. Moon, K. Takatsu, Y. Nakanishi, A. Yoshimura, Spred-1 negatively regulates allergen-induced airway eosinophilia and hyperresponsiveness, J. Exp. Med. 201 (2005) 73–82.
[21] J. Hoeck, M. Woisetschlager, STAT6 mediates eotaxin-1 expression in IL-4 or TNF-alpha-induced fibroblasts, J. Immunol. 166 (2001) 4507–4515.
[22] S. Matsukura, C. Stellato, S.N. Georas, V. Casolaro, J.R. Plitt, K. Miura, S. Kurosawa, U. Schindler, R.P. Schleimer, Interleukin-13 upregulates eotaxin expression in airway epithelial cells by a stat6-dependent mechanism, Am. J. Respir. Cell Mol. Biol. 24 (2001) 755–761.
[23] J. Bernard, D. Treton, C. Vermot-Desroches, C. Boden, P. Horellou, E. Angevin, P. Galanaud, J. Wijdenes, Y. Richard, Expression of interleukin 13 receptor in glioma and renal cell carcinoma: IL-13Ralpha2 as a decoy receptor for IL-13, Lab Invest. 81 (2001) 1223–1231.
[24] J. Arribas, A. Borroto, Protein ectodomain shedding, Chem. Rev. 102 (2002) 4627–4638.
[25] N.M. Hooper, E.H. Karran, A.J. Turner, Membrane protein secretases, Biochem. J. 321 (Pt 2) (1997) 265–279.
[26] J.J. Peschon, J.L. Slack, P. Reddy, K.L. Stocking, S.W. Sunnarborg, D.C. Lee, W.E. Russell, B.J. Castner, R.S. Johnson, J.N. Fitzner, R.W. Boyce, N. Nelson, C.J. Kozlosky, M.F. Wolfson, C.T. Rauch, D.P. Cerretti, R.J. Paxton, C.J. March, R.A. Black, An essential role for ectodomain shedding in mammalian development, Science 282 (1998) 1281–1284.
[27] N.E. King, N. Zimmermann, S.M. Pope, P.C. Fulkerson, N.M. Nikolaidis, A. Mishra, D.P. Witte, M.E. Rothenberg, Expression and regulation of a disintegrin and metalloproteinase (ADAM) 8 in experimental asthma, Am. J. Respir. Cell Mol. Biol. 31 (2004) 257–265.
[28] T. Zheng, Z. Zhu, Z. Wang, R.J. Homer, B. Ma, R.J. Riese Jr., H.A. Chapman Jr., S.D. Shapiro, J.A. Elias, Inducible targeting of IL-13 to the adult lung causes matrix metalloproteinase- and cathepsin-dependent emphysema, J. Clin. Invest. 106 (2000) 1081–1093.
[29] S. Lanone, T. Zheng, Z. Zhu, W. Liu, C.G. Lee, B. Ma, Q. Chen, R.J. Homer, J. Wang, L.A. Rabach, M.E. Rabach, J.M. Shipley, S.D. Shapiro, R.M. Senior, J.A. Elias, Overlapping and enzyme-specific contributions of matrix metalloproteinases-9 and -12 in IL-13-induced inflammation and remodeling, J. Clin. Invest. 110 (2002) 463–474.
[30] Y. Tabata, W. Chen, M.R. Warrier, A.M. Gibson, M.O. Daines, G.K. Hershey, Allergy-driven alternative splicing of IL-13 receptor alpha2 yields distinct membrane and soluble forms, J. Immunol. 177 (2006) 7905–7912.
[31] F.I. Hawari, F.N. Rouhani, X. Cui, Z.X. Yu, C. Buckley, M. Kaler, S.J. Levine, Release of full-length 55-kDa TNF receptor 1 in exosome-like vesicles: a mechanism for generation of soluble cytokine receptors, Proc. Natl. Acad. Sci. USA 101 (2004) 1297–1302.
[32] M.O. Daines, Y. Tabata, B.A. Walker, W. Chen, M.R. Warrier, S. Basu, G.K. Hershey, Level of expression of IL-13R alpha 2 impacts receptor distribution and IL-13 signaling, J. Immunol. 176 (2006) 7495–7501.

Available online at www.sciencedirect.com
ScienceDirect
Comparative Immunology, Microbiology & Infectious Diseases ▮ (▮▮▮▮) ▮▮▮–▮▮▮
C OMPARATIVE I MMUNOLOGY M ICROBIOLOGY & I NFECTIOUS D ISEASES
www.elsevier.com/locate/cimid

Comparative aspects on the role of polypyrimidine tract-binding protein in internal initiation of hepatitis C virus and picornavirus RNAs

T. Nishimura[a,e], M. Saito[a], T. Takano[a,b,c], A. Nomoto[d], M. Kohara[b], K. Tsukiyama-Kohara[a,b,c,*]

[a]*Department of Experimental Phylaxiology, Faculty of Medical and Pharmaceutical Sciences, Kumamoto University 1-1-1, Honjo, Kumamoto 860-8556, Japan*
[b]*Department of Microbiology and Cell Biology, The Tokyo Metropolitan Institute of Medical Science, Tokyo 113-8613, Japan*
[c]*Laboratory Animal Research Center, Institute of Medical Science, The University of Tokyo, Tokyo 108-8639, Japan*
[d]*Graduate School of Medicine, The University of Tokyo, Tokyo 113-0033, Japan*
[e]*The Chemo-Sero-Therapeutic Research Institute, Tokyo 869-1298, Japan*

Accepted 6 July 2007

Abstract

We compared the effects of polypyrimidine tract-binding protein (PTB) on hepatitis C virus (HCV genotype IIa), encephalomyocarditis virus (EMCV) and poliovirus internal ribosome entry site (IRES) activities *in vitro*. It bound strongly to EMCV IRES, but weakly to PV and HCV RNAs. PV IRES showed the strongest dependency to PTB and it showed less than one-tenth of IRES activity after the immuno-depletion of PTB from HeLa S10 lysate with pre-coated anti-PTB IgG beads, comparing to the normal IgG beads-treated S10 lysate. EMCV IRES activity was approximately 40% of that of normal control after PTB depletion.

*Corresponding author. Department of Experimental Phylaxiology, Faculty of Medical and Pharmaceutical Sciences, Kumamoto University 1-1-1, Honjo, Kumamoto 860-8556, Japan.
Tel./fax: +81 96 373 5560.
E-mail address: kkohara@kumamoto-u.ac.jp (K. Tsukiyama-Kohara).

0147-9571/$ - see front matter
doi:10.1016/j.cimid.2007.07.002

Please cite this article as: Nishimura T, et al. Comparative aspects on the role of polypyrimidine tract-binding protein.... Comparat Immunol Microbiol Infect Dis. (2007), doi:10.1016/j.cimid.2007.07.002

Especially, HCV IRES activity was approximately 95%, and most weekly affected by the depletion of PTB. Repletion of PTB to depleted S10 lysate restored activities of PV and EMCV IRESs. The data suggest that PTB plays an important role in picornaviral IRESs, but not in HCV IRES.

Keywords: PTB; HCV; IRES; EMCV; PV; HeLa

Résumé

Dans notre étude, nous avons comparé les effet de la 'polypyrimidine track-binding' (PTB) virus de l'hépatite C (génotype IIa) et l'activité du virus encéphalomyodardite (EMCV) et de l'IRES du poliovirus *in vitro*. La PTB se fixe de manière résistante à l'IRES de l'EMCV mais de manière fragile à l'ARN du PV et du VHC. L'IRES du PV montre la dépendance la plus forte à la PTB et il montre une activité d'IRES de moins de un dixième après immuno-déplétion de la PTB du lysat HeLa10 par des billes d'IgG anti-PTB prêtes à l'emploi, par rapport au HeLa10 traité par des billes d'IgG normales. L'activité de l'IRES de l'EMCV était approximativement égale à 40% de celle sous contrôle normal après déplétion de la PTB. L'activité de l'IRES du VHC était approximativement égale à 95% et la moins sensible à la déplétion de la PTB. La réplétion de la PTB au lysat S10 appauvri rétablit les activités des IRES du PV et de l'EMCV. Les données suggèrent que la PTB joue un rôle important dans les IRES picornaviraux mais pas dans les IRES du VHC. De plus,

Mots clés: PTB; VHC; PTB; IRES; PV; HeLa

1. Introduction

Hepatitis C virus (HCV) possesses a single-stranded RNA (approximately 9610 nucleotides), and classified into the family *Flaviviridae* [1–4]. HCV is a major causative agent of non-A non-B hepatitis, and likely progresses into the chronic hepatitis, cirrhosis and hepatocellular carcinoma.

The 5′ untranslated region (5′UTR) of HCV RNA genome is 341 nucleotides and an internal ribosome entry site (IRES) has been proven to exist in this region [5]. Activities of IRESs of HCV were different from each genotype, and genotype IIa showed almost two-fold higher IRES activity than genotype Ib [6,7].

The IRESs have been discovered in the *Picornavirus* genomes and have a complex RNA secondary structure [5,8]. The importance of secondary structure to IRES function is understood by studies that sequence substitutions within the IRES are accompanied by compensatory mutations that act to maintain the RNA secondary structure. The 40S ribosome subunit is recruited within these IRES without binding to the m^7G cap and eIF4E [9,10]. IRESs can be classified into at least 3 groups, according to their features. IRESs derived from entero- and rhinoviruses are classified into type 1(poliovirus), and oligopyrimidine tract is located in 50–100 nucleotides past the 3′ end of the IRES [11,12]. The oligopyrimidine tract

Please cite this article as: Nishimura T, et al. Comparative aspects on the role of polypyrimidine tract-binding protein.... Comparat Immunol Microbiol Infect Dis. (2007), doi:10.1016/j.cimid.2007.07.002

immediately follows the 3′ end of type 2 (cardio- and aphthoviruses) IRES. Encephalomyocarditis virus (EMCV) and foot and mouse disease virus possess type 2 IRESs and utilyzes eIF4G and 4B [13,14]. The HCV and classical swine fever virus (CSFV) possess type 3 IRESs which interact directly to 40S ribosome subunit and eIF3 [15]. In addition to the requirement for eIF in each IRESs, the existence of internal initiation trans-acting factors (ITAFs) has been reported [16,17]. One of ITAFs binds to picornavirus and HCV IRES commonly is polypyrimidine tract-binding protein (PTB) [11,18-20]. PTB may work in each IRESs, however, its exact role in internal initiation has been still unclear at present. In the present study, requirement of PTB in poliovirus, EMCV and HCV IRESs has been characterized, and compared in *in vitro* translation system by depletion and complementation of PTB.

2. Materials and methods

2.1. Isolation of cDNA clones and construction of expression vectors

HCV cDNA that corresponds to nucleotide positions 1-418 (GenBank) was isolated by PCR from plasma of HCV type IIa infected patients [5], using a sense primer, 5′-GATCTAGAGCCCGCCCCCTGATGGGGGCGA-3′, and antisense primer 5′-TGTCCTGCAGTTCAAGGGCCC-3′. The amplified cDNA was digested with XbaI and AatII, and replaced with an XbaI and AatII fragment (5′UTR) of pkIV [5]. A whole cDNA which was excised by XbaI-HindIII was filled up with Klenow fragment (Takara) and cloned into StuI site of pNar3 [5], and the resulting plasmid was designated as pNII5′.

Poliovirus cDNA expression vector T7M2, CAT gene with 5′UTR of EMCV (pBSECAT) and T7CAT were constructed, as described previously [19,21].

PTB cDNA that encodes whole coding region (amino acids no. 1-531) [22] or C terminal half (amino acids no. 291-531) of PTB was synthesized by RT-PCR, and cloned into the downstream of glutathione S transferase (GST) protein in frame in pGEX-KG vector, and was designated as pGST-PTB.

2.2. Expression of PTB and production of specific antibodies

The pGST-PTB was transformed in *Esherichia coli* strain SCS-1 and induced expression with 1 mM IPTG induction. *E. coli* culture (40 ml) was peletted by centrifuge and lyzed with lysozyme (1 mg/ml) and sonicated with 1% TritonX100 and 10 mM DTT. The supernatant was reacted to Glutathione Sepharose 4B (Amersham Bioscience), cleaved by thrombin (SIGMA) and purified with ploy U Sepharose 4B (Amersham Bioscience), as described previously [22]. Rabbits or guinea pigs immunized were over four times intradermal and subcutaneously or intraperitonealy with purified recombinant whole or C-terminal half of PTB (200 μg). These hyperimmune sera were purified by the protein G Sepharose 4B (Amersham Bioscience). The anti PTB rabbit IgG was further purified by the affinity

Please cite this article as: Nishimura T, et al. Comparative aspects on the role of polypyrimidine tract-binding protein.... Comparat Immunol Microbiol Infect Dis. (2007), doi:10.1016/j.cimid.2007.07.002

column of PTB cross-linking Formyl Cellulofine (Seikagaku Kogyo Co.), as described by manufacturer's instruction manual.

2.3. UV cross-linking assays and immunoprecipitation

RNA probes corresponding to nucleotide(nt.) 1-341 of the HCV 5'UTR, nt. 260-833 of the EMCV 5'UTR and nt. 1-747 of the PV 5'UTR were generated by the digestion of pNII5' with BspHI, pBSECAT with BalI and pM1(T7) with HgiAI, respectively, and transcribed by using Megascript™ T7 RNA polymerase kit (Ambion) with [α-^{32}P]UTP (NEN). Labelled RNA probes were purified by the Nuc Trap™ push columns (Stratagene). Probes ($1-5 \times 10^6$ cpm) were incubated with or without competitor RNA in HeLa S10 lysate (10 μg) at 30 °C for 20 min and irradiated on ice for 20 min in a UV Stratalinker (Stratagene). Unbound RNAs were digested with 10 μg of RNase A (Sigma), 200 units of RNase T1 (Gibco BRL) and 1 unit of phosphodiesterase I (Amersham Bioscience). Samples were analyzed by SDS-PAGE and dried gel was exposed to imaging plate (Fuji) or X-ray film (Kodak). Radioactivity was measured by the Bio-image analyzer BAS 2000 (Fuji).

HeLa S10 or recombinant PTB which was UV cross-linked to labeled HCV RNA was solubilyzed by single lysis buffer containing 1% NP40, reacted with affinity-purified anti-PTB Ig (4 μg) and precipitated by affigel protein A (Bio Rad) beads. Precipitated protein was further characterized by SDS-PAGE.

2.4. Immuno-depletion test

Affigel protein A (Bio Rad) 50 μl was pretreated with HeLa S10 100 μl at 37 °C for 1 h. The affinity purified anti-PTB Rabbit IgG (500 μg) was added, and rotated at room temperature for 3 h. These IgG beads were coated by 10% FCS-0.1 M phosphate buffer (pH 8.0) at 37 °C for 1 h, washed with S10 dialysis buffer (10 mM Hepes-KOH pH7.5, 90 mM KOAc, 1.5 mM $Mg(OAc)_2$), and reacted to HeLa S10 lysate (150 μl) at 4 °C overnight. The supernatants of each reaction were utilized for *in vitro* translation.

2.5. Competitive ELISA

Serocluster 'U' vinyl plate with 96 wells (Costar) was coated with affinity purified rabbit anti-PTB-C term IgG (2.5 μg/ml) at 4 °C overnight. After blocking with 1% casein PBS (−) at 25 °C for 2 h, non-treated or immunodepleted HeLa S10 lysate were added to each well, and incubate at 25 °C for 2 h. Purified recombinant PTB was used for standard and non-treated or immunodepleted HeLa S10 lysates were added to each well, and incubate at 25 °C for 2 h. Then anti-PTB guinea pig IgG (1 μg/ml) was reacted at 37 °C for 1 h, and finally anti-guineapig -IgG HRP (Dako 1:2000) was reacted at 37 °C for 1 h. *Ortho*-phenylene diamine was added to each well as substrate, and the absorbance was measured by microplate reader Model 450 (Bio Rad).

Please cite this article as: Nishimura T, et al. Comparative aspects on the role of polypyrimidine tract-binding protein.... Comparat Immunol Microbiol Infect Dis. (2007), doi:10.1016/j.cimid.2007.07.002

2.6. In vitro transcription and translation

Plasmids were linearized by digestion with XmnI (pNII5′), HpaI (pBSECAT) and NheI (p(M1)T7) and transcribed into RNA by Megascript™ T7 RNA polymerase kit (Ambion). RNAs were treated with DNase I, precipitated with LiCl, and quantitated by the Spectrophotometer DU64 (Beckman).

Synthetic RNAs (pNII5′ RNA; 1.0 pmol, pBSECAT; 1.8 pmol, p(M1)T7; 0.36 pmol and they were optimized for the linear phase in translation activity) were translated in HeLa S10 lysates at 37 °C for 30 min with [^{35}S]-Methionine (ICN), as described previously[5] . Translation products were analyzed using 7.5–15% gradient SDS-PAGE.

2.7. Restoration assay

Purified recombinant PTB, bovine serum albumin and ribosome salt wash (RSW) were dialyzed to S10 dialysis buffer, and added to PTB depleted or non-treated HeLa S10. RSW (total 6.7 ml) was prepared from 6.11 of HeLa S10, as described previously [5] (kindly supplied by Dr. H. Toyoda).

3. Results

3.1. Fifty-seven and 60 kDa doublet protein bound HCV, EMCV and PV RNA

HeLa cytoplasmic proteins that were detected by UV cross-linking to ^{32}P-UTP labeled RNA derived from the HCV, EMCV, and PV 5′UTR were compared (Fig. 1). Total counts of binding proteins in HCV RNA was five times lower than those of EMCV RNA, and three times lower than those of PV-RNA (PSL; HCV 21536.9, EMCV 105622.8, PV 59307.9). Among these cytoplasmic proteins, 57 and 60 kDa doublet bands on HCV RNA,EMCV RNA and PV RNA have been identified to be PTB (Fig. 1, indicated by asterisk). According to band intensities of the 57 and 60 kDa proteins, PTB bound to EMCV IRES most abundantly, and more diminished amount of PTB bound to PV and HCV IRESs (Fig. 1).

3.2. Identification of P57/60 kDa doublet protein on HCV-RNA as PTB

HCV-IRES-binding proteins with molecular weight of 57/60 kDa were further characterized. The recombinant PTB protein was expressed in *E. coli.* in the presence of IPTG, purified by glutathione sepharose and polyU sepharose column (Fig. 2A), and reacted with affinity purified anti-PTB IgG (Fig. 2B), as described in Section 2. Labeled HCV RNA 5′UTR was cross-linked to HeLa S10 lysate, and immunoprecipitated by affinity purified anti-PTB IgG (Fig. 3). The 57 and 60 kDa doublet bands were specifically reacted to the anti-PTB IgG (Fig. 3, lane HeLa). The recombinant PTB protein was cross-linked with HCV RNA 5′UTR and precipitated with anti-PTB IgG (Fig. 3, lane PTB). These results strongly indicate that PTB

Please cite this article as: Nishimura T, et al. Comparative aspects on the role of polypyrimidine tract-binding protein.... Comparat Immunol Microbiol Infect Dis. (2007), doi:10.1016/j.cimid.2007.07.002

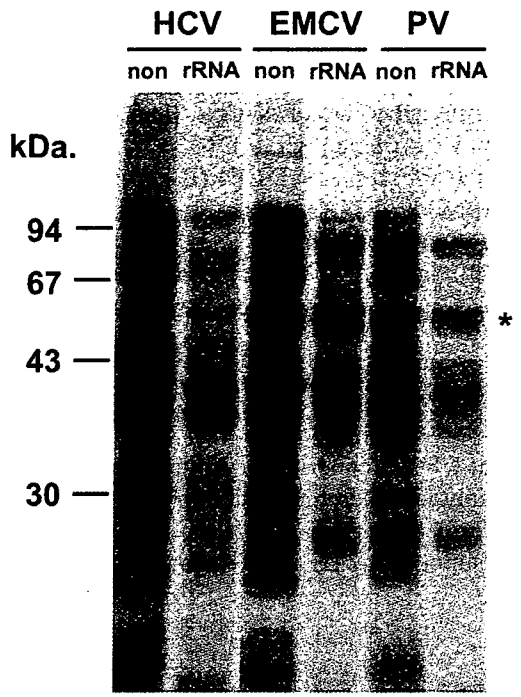

Fig. 1. UV-cross-linking analysis of binding factors to HCV, EMCV and PV-IRES RNAs. Each reaction without competitor indicates "non", and with competitor rRNA indicates rRNA on the top of the lanes. Asterisk indicates the position of PTB proteins. An asterisk indicates PTB binding.

specifically bound to HCV RNA 5′UTR, and observed as doublet protein with molecular weight of 57 and 60 kDa.

3.3. Depletion of PTB in HeLa S10 lysate

Previous results indicated the possibility that other factors than canonical eukaryotic translation initiation factors (eIFs) are working in cap independent translation. PTB is one of the candidates and when the PTB might be commonly used in several kinds of IRESs, it might play the central role in internal initiation. To compare the significance of PTB in translation initiation in HCV and other Picorna virus IRESs, PTB in HeLa S10 lysate was depleted by affinity purified anti-PTB IgG. For the depletion of PTB, pre-coating of Affi-gel protein A beads was necessary to block the non-specific adsorption, as described in Section 2. Pre-coated beads were reacted with anti-PTB IgG. From the preliminary experiments, more than 100 times higher molar ratio of anti-PTB IgG to PTB in S10 lysates was required for the over 90% depletion, as described in Materials and methods. We performed the PTB depletion, and 94.5% of PTB was depleted by anti-PTB IgG and 26.3% of PTB was depleted by pre-immune IgG (Fig. 4). We further examined the effect of PTB

Please cite this article as: Nishimura T, et al. Comparative aspects on the role of polypyrimidine tract-binding protein.... Comparat Immunol Microbiol Infect Dis. (2007), doi:10.1016/j.cimid.2007.07.002

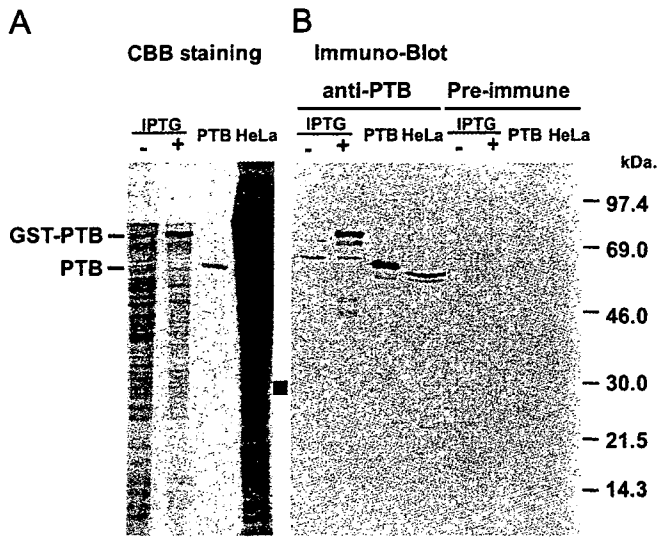

Fig. 2. Expression of recombinant PTB protein fused with GST in *E. coli*: (A) Expression of PTB protein was induced by IPTG, purified by glutathione sepharose column and stained with CBB. (B) Expressed recombinant PTB was transferred to membrane and reacted with specific antibody by WB.

depletion to the binding of cellular factors to three IRESs (Fig. 5). In PTB depleted lysates, binding of 57 and 60 kDa doublet protein was decreased, especially in PV-RNA. However, binding of other factors was not influenced significantly, other than 28 kDa protein (Fig. 5, indicated by an arrow).

3.4. Effect of PTB depletion in translation

Influence of PTB depletion was examined in HCV, EMCV and PV-RNA (Fig. 6A, Table 1). The reaction curves of each RNA were different from each other (data not shown), and the optimum quantity of each RNA used in this study was different from each other (Table 1). From the comparison of translation activity in PTB depleted S10 lysates, translation of PV-RNA was significantly decreased in 4 and 8 μl lysates (22–4.5%, 15–0.9%, Table 1, Fig. 6A). Translation of EMCV-IRES was significantly decreased after PTB depletion (53–44% (4 μl), 28–11% (8 μl)), but this suppression was not as much as PV-IRES. Activity of HCV-IRES was almost similar between pre-immune IgG-treated and anti-PTB IgG-treated S10 lysates. Because the optimal RNA quantities for translation are different in each IRESs, therefore, we calculated the ratio of PTB quantity per template RNA molecules (PTB/RNA) (ng/pmol; Table 1). In PV-IRES, translation activity was significantly reduced after depletion (4.5%, 0.9%) and the PTB/RNA ratio was 1.4 and 0.56. EMCV-IRES and HCV-IRES activity. Influence of PTB depletion to HCV-IRES activity was much lower than those of PV and EMCV.

Please cite this article as: Nishimura T, et al. Comparative aspects on the role of polypyrimidine tract-binding protein.... Comparat Immunol Microbiol Infect Dis. (2007), doi:10.1016/j.cimid.2007.07.002

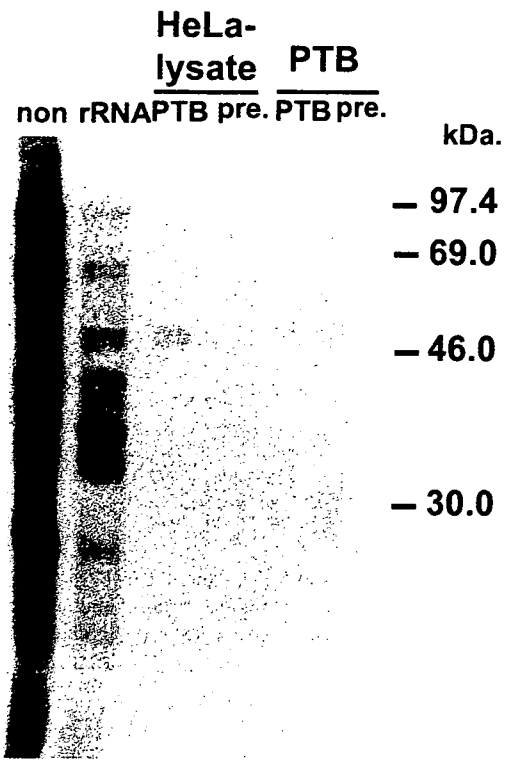

Fig. 3. HCV-IRES cross-linked S10 and PTB was immuno-precipitated by purified anti PTB antibody and pre-immune antibody. The 57 and 60 kDa doublet bands were specifically reacted to the anti-PTB IgG (lane HeLa). The recombinant PTB protein was cross-linked with HCV RNA 5′UTR and precipitated with anti-PTB IgG (lane PTB). Pre-immune antibody did not reacted to both Hela S10 and PTB.

The IRES activity of EMCV and PV-RNA was decreased by treatment of pre-immune IgG, however, treatment of pre-immune IgG did not influence significantly to the IRES activity of HCV-RNA.

3.5. Restoration of PTB to depleted S10

To clarify the effect of immuno-depletion was mainly caused by the decreased quantity of PTB, the purified recombinant PTB or RSW was added to depleted S10 (Fig. 6B). The IRES activity of PV-RNA in depleted S10 lysate (6 μl) was increased by the addition of PTB in dose-dependent manner. The EMCV-IRES activity was recovered even in the presence of 1 μg of PTB in depleted S10 lysate (4.0 μl). When too much quantity of PTB was added to the S10, translation activity of PV, EMCV and HCV decreased (over 10 times of PTB in PV, over 300 times in EMCV and over 500 times in HCV RNA, data not shown).

Translation activity of PV and EMCV-RNA became higher after the addition of RSW to anti-PTB IgG depleted S10 (150% and117%, respectively) (date not

Please cite this article as: Nishimura T, et al. Comparative aspects on the role of polypyrimidine tract-binding protein.... Comparat Immunol Microbiol Infect Dis. (2007), doi:10.1016/j.cimid.2007.07.002

Fig. 4. Depletion of HeLa S10 by pre-immune IgG and affinity purified anti-PTB IgG. They were reacted with anti-PTB antibody by WB. Asterisk indicates the position of PTB proteins. Anti-PTB IgG deplete 94.5% of PTB (lane PTB) and pre-immune IgG deplete 26.3% of PTB (lane pre).

shown). This might indicate the existence of several translation factors other than PTB, which were lost during the treatment of IgG.

Taken together, results of this study strongly indicate that significance of PTB was highest in PV-IRES and was lowest implication in HCV-IRES.

4. Discussion

In present study, the significance of PTB in HCV, EMCV and PV IRESs has been compared. From the immuno-depletion experiment (Table 1), PTB-Ig depleted S10 (4.0 μl) contained 0.009 molecule of PTB per 1 molecule of RNA, in which PV IRES activity is 0.9%. This may indicate that almost one PTB molecule should be required

Please cite this article as: Nishimura T, et al. Comparative aspects on the role of polypyrimidine tract-binding protein.... Comparat Immunol Microbiol Infect Dis. (2007), doi:10.1016/j.cimid.2007.07.002

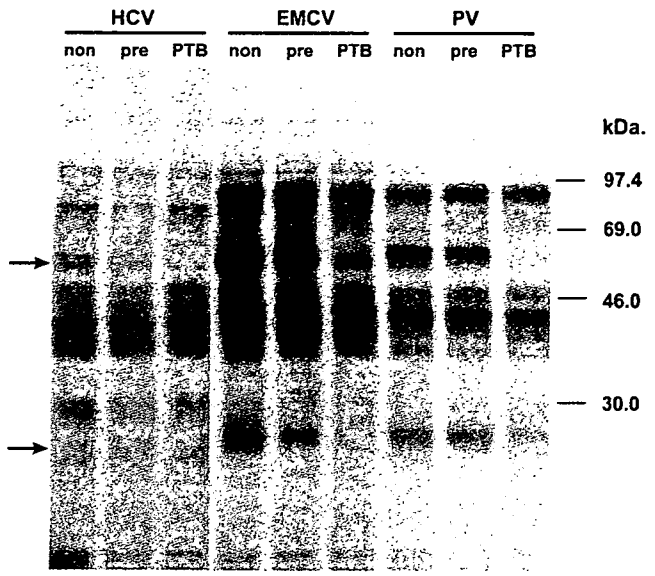

Fig. 5. UV-cross-linking analysis of HCV, EMCV and PV RNA with non-treated, pre-immune IgG-treated, and anti-PTB IgG-treated HeLa S10 lysate (lane non, pre, PTB). Upper arrow indicates the binding of PTB. Doublet protein (57 and 60 kDa) was decreased, especially in PV-RNA. Lower arrow indicates 28 kDa protein.

for 100% activity of PV IRES-RNA. In the case of EMCV IRES-RNA, 0.002 molecule of PTB per RNA gave 11% of EMCV IRES activity, and that of HCV IRES, 0.0025 molecule of PTB gave 31% of HCV IRES activity. Therefore, requirement of PTB for IRES activity was highest in PV, and less in EMCV and HCV IRES-RNA.

From the results in this study, we can compare the requirement amount of PTB in IRES activity with those of canonical eIFs. The most limiting initiation factor in cells is eIF4E, with estimates in rabbit reticulocyte lysates ranging from 0.02 copies [23] to 1 copy [24] per ribosome. The concentration of ribosomes has been estimated to be approximately 2 μM [25]. From the results of *in vitro* translation experiment, PTB should work at 0.1–0.15 M in each IRESs at maximum activity (Table 1). Therefore, working concentration of PTB for IRES activity should show almost similar to those of eIFs.

During the immuno-depletion experiment, treatment of normal IgG conjugated beads decreased the IRESs activity; 89 (6.5 μl) or 33 (3.5 μl)% in HCV IRES, 53 or 28% in EMCV IRES, and 22% or 15% in PV-IRES (Table 1). This may suggest the existence of unknown factors, which could be inactivated during the process of immuno-depletion experiment, and these effects in PV-IRES were highest among the IRESs. PV-IRES is classified into the type I [26], and the canonical eIFs with the exception of cap-binding protein eIF4E [27] and PTB [26], La [26] and 39 kDa poly(rC)-binding protein [26] are working. In EMCV IRES (type II), eIF4G was

Please cite this article as: Nishimura T, et al. Comparative aspects on the role of polypyrimidine tract-binding protein.... Comparat Immunol Microbiol Infect Dis. (2007), doi:10.1016/j.cimid.2007.07.002

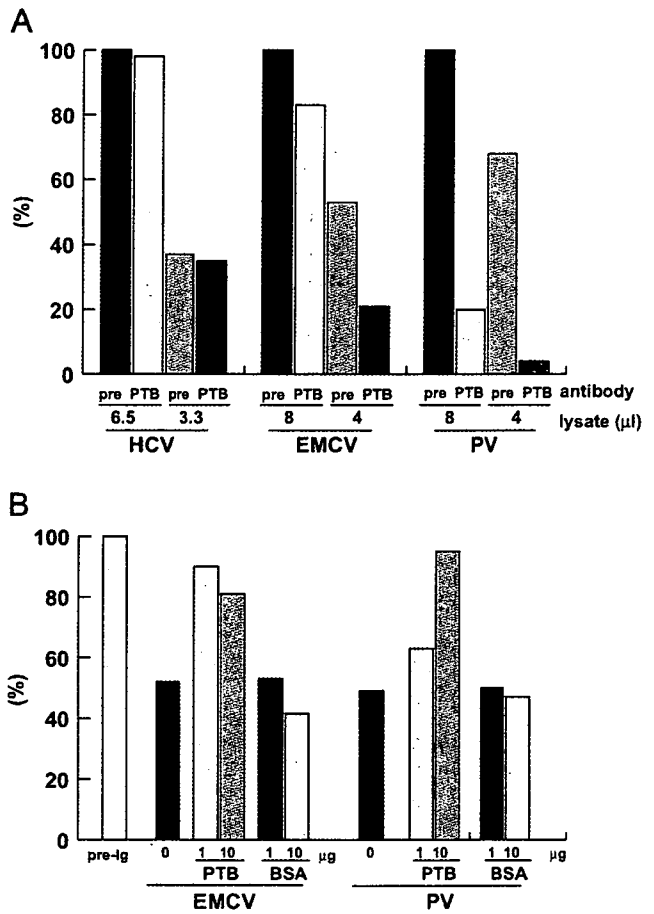

Fig. 6. (A) Effect of PTB depletion in HCV, EMCV and PV IRES. IRESs were translated in pre-immune IgG-depleted and anti-PTB IgG depleted S10 lysates (3.3, 6.5 μl in HCV-IRES, 4.0, 8.0 μl in EMCV- and PV-IRES. Translated products in SDS-PAGE were measured by image analyzer, and the quantity (PSL) of pre-immune IgG-treated S10 lysate was calculated as 100%. (B) Recovery of translation in PTB depleted S10 lysate by addition of recombinant PTB protein (1 and 10 μg. Translated products in SDS-PAGE were measured by image analyzer, and the quantity (PSL) of pre-immune IgG-treated S10 lysate was calculated as 100%.

directly bound and eIF4A and eIF4B can recruit 43S preinitiation complex which is composed of 40S ribosomal subunit and eIF3, eIF2, GTP and initiator tRNA[13]. Recent findings indicated the dependence of EMCV IRES on PTB for activity [28]. The HCV IRES possesses striking difference from type I and II IRESs, it recruits 43S preinitiation complex to initiation codon to form a 48S complex without involvement of eIF4A, 4B or 4F [29]. Thus, HCV IRES is simple and does not require most of eIFs, and might not be influenced by the depletion experiment using normal IgGs.

Please cite this article as: Nishimura T, et al. Comparative aspects on the role of polypyrimidine tract-binding protein.... Comparat Immunol Microbiol Infect Dis. (2007), doi:10.1016/j.cimid.2007.07.002

Table 1
Effect of PTB depletion in HCV, EMCV and PV IRES

RNA	RNA quantity (pmol)	S10 (μl)	PTB (ng)	Molar ratio of PTB to RNA	Ratio of translation (%)[a]
HCV	1.0	*Untreated*			
		6.5	7.2	0.12	100
		3.5	3.6	0.06	63
		Pre-im.-IgG			
		6.5	5.2	0.085	89
		3.5	2.6	0.045	33
		αPTB-IgG			
		6.5	0.4	0.005	87
		3.5	0.2	0.0025	31
EMCV	1.8	*Untreated*			
		8.0	8.8	0.08	100
		4.0	4.4	0.04	57
		Pre-im.-IgG			
		8.0	6.4	0.06	53
		4.0	3.2	0.03	28
		αPTB-IgG			
		8.0	0.5	0.005	44
		4.0	0.2	0.002	11
PV	0.36	*Untreated*			
		8.0	8.8	0.4	100
		4.0	4.4	0.2	65
		Pre-im.-IgG			
		8.0	6.4	0.3	22
		4.0	3.2	0.15	15
		αPTB-IgG			
		8.0	0.5	0.02	4.5
		4.0	0.2	0.009	0.9

[a]Ratio of translation products was quantitated by image analyzer.

Recent riboproteomic approach revealed the novel interacting proteins to IRESs [30], other than PTB, such as actin, forming homolog overexpressed in spleen, and microtuble interacting protein that associates with TRAF3. These factors should be characterized as novel ITAFs and comparative aspects in different IRESs should be addressed in the future work to clarify the character of each IRESs.

Acknowledgments

This work was supported by the grants from the Ministry of Health and Welfare, or Education, Culture, Sports, Science and Technology of Japan, the program for

Please cite this article as: Nishimura T, et al. Comparative aspects on the role of polypyrimidine tract-binding protein.... Comparat Immunol Microbiol Infect Dis. (2007), doi:10.1016/j.cimid.2007.07.002

promotion of fundamental studies in health sciences of the National Institute of Biomedical Innovation, and the Cooperative Research Project on Clinical and Epidemiological Studies of Emerging and Re-emerging Infectious Diseases.

References

[1] Choo QL, Kuo G, Weiner AJ, Overby LR, Bradley DW, Houghton M. Isolation of a cDNA clone derived from a blood-borne non-A, non-B viral hepatitis genome. Science 1989;244:359–62.
[2] Takamizawa A, Mori C, Fuke I, Manabe S, Murakami S, Fujita J, et al. Structure and organization of the hepatitis C virus genome isolated from human carriers. J Virol 1991;65:1105–13.
[3] Kato N, Hijikata M, Ootsuyama Y, Nakagawa M, Ohkoshi S, Sugimura T, et al. Molecular cloning of the human hepatitis C virus genome from Japanese patients with non-A, non-B hepatitis. Proc Natl Acad Sci USA 1990;87:9524–8.
[4] Kaito M, Watanabe S, Tsukiyama-Kohara K, Yamaguchi K, Kobayashi Y, Konishi M, et al. Hepatitis C virus particle detected by immunoelectron microscopic study. J Gen Virol 1994;75(Part 7):1755–60.
[5] Tsukiyama-Kohara K, Iizuka N, Kohara M, Nomota A. Internal ribosome entry site within hepatitis C virus RNA. J Virol 1992;66:1476–83.
[6] Kamoshita N, Tsukiyama-Kohara K, Kohara M, Nomoto A. Genetic analysis of internal ribosomal entry site on hepatitis C virus RNA: implication for involvement of the highly ordered structure and cell type-specific transacting factors. Virology 1997;233:9–18.
[7] Nomoto A, Tsukiyama-Kohara K, Kohara M. Mechanism of translation initiation on hepatitis C virus RNA. Princess Takamatsu Symp 1995;25:111–9.
[8] Pelletier J, Sonenberg N. Internal initiation of translation of eukaryotic mRNA directed by a sequence derived from poliovirus RNA. Nature 1988;334:320–5.
[9] Kieft JS, Zhou K, Jubin R, Doudna JA. Mechanism of ribosome recruitment by hepatitis C IRES RNA. RNA 2001;7:194–206.
[10] Yu Y, Ji H, Doudna JA, Leary JA. Mass spectrometric analysis of the human 40S ribosomal subunit: native and HCV IRES-bound complexes. Protein Sci 2005;14:1438–46.
[11] Hellen CU, Pestova TV, Litterst M, Wimmer E. The cellular polypeptide p57 (pyrimidine tract-binding protein) binds to multiple sites in the poliovirus 5′ nontranslated region. J Virol 1994;68:941–50.
[12] Hunt SL, Jackson RJ. Polypyrimidine-tract binding protein (PTB) is necessary, but not sufficient, for efficient internal initiation of translation of human rhinovirus-2 RNA. RNA 1999;5:344–59.
[13] Kolupaeva VG, Pestova TV, Hellen CU, Shatsky IN. Translation eukaryotic initiation factor 4G recognizes a specific structural element within the internal ribosome entry site of encephalomyocarditis virus RNA. J Biol Chem 1998;273:18599–604.
[14] Kolupaeva VG, Hellen CU, Shatsky IN. Structural analysis of the interaction of the pyrimidine tract-binding protein with the internal ribosomal entry site of encephalomyocarditis virus and foot-and-mouth disease virus RNAs. RNA 1996;2:1199–212.
[15] Sizova DV, Kolupaeva VG, Pestova TV, Shatsky IN, Hellen CU. Specific interaction of eukaryotic translation initiation factor 3 with the 5′ nontranslated regions of hepatitis C virus and classical swine fever virus RNAs. J Virol 1998;72:4775–82.
[16] Witherell GW, Wimmer E. Encephalomyocarditis virus internal ribosomal entry site RNA–protein interactions. J Virol 1994;68:3183–92.
[17] Scheper GC, Voorma HO, Thomas AA. Binding of eukaryotic initiation factor-2 and trans-acting factors to the 5′ untranslated region of encephalomyocarditis virus RNA. Biochimie 1994;76:801–9.
[18] Ali N, Siddiqui A. Interaction of polypyrimidine tract-binding protein with the 5′ noncoding region of the hepatitis C virus RNA genome and its functional requirement in internal initiation of translation. J Virol 1995;69:6367–75.
[19] Jang SK, Wimmer E. Cap-independent translation of encephalomyocarditis virus RNA: structural elements of the internal ribosomal entry site and involvement of a cellular 57-kDa RNA-binding protein. Genes Dev 1990;4:1560–72.

Please cite this article as: Nishimura T, et al. Comparative aspects on the role of polypyrimidine tract-binding protein.... Comparat Immunol Microbiol Infect Dis. (2007), doi:10.1016/j.cimid.2007.07.002

[20] Luz N, Beck E. Interaction of a cellular 57-kDa protein with the internal translation initiation site of foot-and-mouth disease virus. J Virol 1991;65:6486–94.
[21] Jang SK, Pestova TV, Hellen CU, Witherell GW, Wimmer E. Cap-independent translation of picornavirus RNAs: structure and function of the internal ribosomal entry site. Enzyme 1990;44:292–309.
[22] Garcia-Blanco MA, Jamison SF, Sharp PA. Identification and purification of a 62,000-Da protein that binds specifically to the polypyrimidine tract of introns. Genes Dev 1989;3:1874–86.
[23] Hiremath LS, Webb NR, Rhoads RE. Immunological detection of the messenger RNA cap-binding protein. J Biol Chem 1985;260:7843–9.
[24] Rau M, Ohlmann T, Morley SJ, Pain VM. A reevaluation of the cap-binding protein, eIF4E, as a rate-limiting factor for initiation of translation in reticulocyte lysate. J Biol Chem 1996;271:8983–90.
[25] Duncan R, Hershey JW. Identification and quantitation of levels of protein synthesis initiation factors in crude HeLa cell lysates by two-dimensional polyacrylamide gel electrophoresis. J Biol Chem 1983;258:7228–35.
[26] Flint SJ, Enquist LW, Krug RM, Racaniello VR, Skalka AM, editors. Virology. Washington, DC: ASM Press; 2000.
[27] Gingras AC, Svitkin Y, Belsham GJ, Pause A, Sonenberg N. Activation of the translational suppressor 4E-BP1 following infection with encephalomyocarditis virus and poliovirus. Proc Natl Acad Sci USA 1996;93:5578–83.
[28] Kaminski A, Jackson RJ. The polypyrimidine tract binding protein (PTB) requirement for internal initiation of translation of cardiovirus RNAs is conditional rather than absolute. RNA 1998;4:626–38.
[29] Hellen CU, Pestova TV. Translation of hepatitis C virus RNA. J Viral Hepat 1999;6:79–87.
[30] Lu H, Li W, Noble WS, Payan D, Anderson DC. Riboproteomics of the hepatitis C virus internal ribosomal entry site. J Proteome Res 2004;3:949–57.

Please cite this article as: Nishimura T, et al. Comparative aspects on the role of polypyrimidine tract-binding protein.... Comparat Immunol Microbiol Infect Dis. (2007), doi:10.1016/j.cimid.2007.07.002